

THE STATISTICS OF RADIO ASTRONOMICAL POLARIMETRY: BRIGHT SOURCES AND HIGH TIME RESOLUTION

W. VAN STRATEN

Centre for Astrophysics and Supercomputing, Swinburne University of Technology,
 Hawthorn, VIC 3122, Australia

ABSTRACT

A four-dimensional statistical description of electromagnetic radiation is developed and applied to the analysis of radio pulsar polarization. The new formalism provides an elementary statistical explanation of the modal broadening phenomenon in single pulse observations. It is also used to argue that the degree of polarization of giant pulses has been poorly defined in past studies. Single and giant pulse polarimetry typically involves sources with large flux densities and observations with high time resolution, factors that necessitate consideration of source-intrinsic noise and small-number statistics. Self noise is shown to fully explain the excess polarization dispersion previously noted in single pulse observations of bright pulsars, obviating the need for additional randomly polarized radiation. Rather, these observations are more simply interpreted as an incoherent sum of covariant, orthogonal, partially polarized modes. Based on this premise, the four-dimensional covariance matrix of the Stokes parameters may be used to derive mode-separated pulse profiles without any assumptions about the intrinsic degrees of mode polarization. Finally, utilizing the small-number statistics of the Stokes parameters, it is established that the degree of polarization of an unresolved pulse is fundamentally undefined; therefore, previous claims of highly polarized giant pulses are unsubstantiated. Unpublished supplementary material is appended after the bibliography.

Keywords: methods: data analysis — methods: statistical — polarization — pulsars: general — techniques: polarimetric

1. INTRODUCTION

Radio pulsars exhibit dramatic fluctuations in total and polarized flux densities on a diverse range of longitudinal, temporal and spectral scales. As a function of pulse phase, both average profiles and sub-pulses make sudden transitions between orthogonally polarized modes (e.g. [Taylor et al. 1971](#); [Manchester et al. 1975](#)). The radiation at a single pulse phase often appears as an incoherent superposition of modes, both orthogonal and non-orthogonal (e.g. [Backer & Rankin 1980](#); [McKinnon 2003a](#)). Evidence has also been presented for variations that may indicate stochastic generalized Faraday rotation in the pulsar magnetosphere ([Edwards & Stappers 2004](#)).

In an extensive study of single-pulse polarization fluctuations at 1400 MHz, [Stinebring et al. \(1984\)](#) observed that histograms of the linear polarization position angle were broader than could be explained by instrumental noise alone. This modal broadening of

the position angle distribution was interpreted as evidence of a superposed randomized emission component. [McKinnon & Stinebring \(1998\)](#) revisited the issue with a statistical model that described correlated intensity fluctuations of completely polarized orthogonal modes. Although the predicted position angle distributions were qualitatively similar to the observations, the measured histograms were wider than those produced by a numerical simulation of modal broadening that included instrumental noise. Source-intrinsic noise was later used to explain the excess polarization scatter of bright pulses in an analysis of mode-separated profiles ([McKinnon & Stinebring 2000](#)); however, it was given no further consideration in all subsequent statistical treatments by [McKinnon \(2002, 2003b, 2004, 2006\)](#).

These begin with the reasonable assumptions that the instantaneous signal-to-noise ratio S/N is low and a sufficiently large number of samples have been averaged, such that the stochastic noise in all four Stokes parameters can be treated as uncorrelated and normally distributed. These assumptions form part of the three-dimensional eigenvalue analyses of the Stokes polarization vector by [McKinnon \(2004\)](#) and

Edwards & Stappers (2004). As in Stinebring et al. (1984), these studies concluded that modal broadening is due to the incoherent addition of randomly polarized radiation that is intrinsic to the pulsar. The basic premises of these experiments are valid for the vast majority of pulsar observations; however, they become untenable for the bright sources on which these studies focus. That is, when the instantaneous $S/N \gtrsim 1$, the Stokes polarization vector can no longer be treated in isolation and the correlated self noise intrinsic to all four stochastic Stokes parameters must be accounted.

These considerations are particularly relevant to the study of giant pulses. Those from the Crab pulsar reach brightness temperatures in excess of 10^{37} Kelvin and remain unresolved in observations with nanosecond resolution (Hankins et al. 2003). Consequently, previous analyses of giant pulses have typically presented polarization data at the sampling resolution of the instrument; that is, where the time-bandwidth product is of the order of unity. For example, Heiles et al. (1970) studied giant pulses from the Crab pulsar using an instrument with bandwidth, $\delta\nu = 8.3$ kHz, and presented plots of the Stokes parameters at a resolution of $\tau = 120\mu\text{s}$. Cognard et al. (1996) plotted the total intensity and circular polarization of the strongest giant pulse and interpulse observed from PSR B1937+21 with $\tau = 1.2\mu\text{s}$ and $\delta\nu = 500$ kHz. Using a baseband recorder with $\delta\nu = 500$ MHz, Hankins et al. (2003) plotted the intensities of left and right circularly polarized radiation from Crab giant pulses at a time resolution of 2 ns. Each of these studies concluded that giant pulses are highly polarized. However, in each experiment, $\tau\delta\nu \sim 1$; at this resolution, every discrete sample of the electric field is completely polarized, regardless of the intrinsic degree of polarization of the source. That is, the instantaneous degree of polarization is fundamentally undefined.

To study the polarization of intense sources of impulsive radiation at high time resolution, it is necessary to consider averages over small numbers of samples and source-intrinsic noise statistics. These limitations are given careful attention in the statistical theory of polarized shot noise (Cordes 1976). This seminal work enables characterization of the timescales of microstructure polarization fluctuations via the auto-correlation functions of the total intensity and degrees of linear and circular polarization (e.g. Cordes & Hankins 1977). It has also been extended to study the degree of polarization via the cross-correlation as a function of time lag between the instantaneous total intensity spectra of giant pulses (Cordes et al. 2004).

This paper presents a complimentary approach based on the four-dimensional joint distribution and covariance matrix of the Stokes parameters, with emphasis placed on the statistical degrees of freedom of the un-

derlying stochastic process. Relevant theoretical results are drawn from various sources, ranging from studies of the scattering of monochromatic light in optical fibres (e.g. Steeger et al. 1984) to the classification of synthetic aperture radar images (e.g. Touzi & Lopes 1996).

Following a brief review of polarization algebra in § 2, the joint probability density functions of the Stokes parameters at different resolutions are derived in § 3, where the results are compared and contrasted with previous works. The formalism is related to the study of radio pulsar polarization in § 4, where the effects of amplitude modulation and wave coherence on the degrees of freedom of the pulsar signal are discussed. Finally, the results are utilized to reexamine past statistical analyses of orthogonally polarized modes, randomly polarized radiation, and giant pulse polarimetry. It is concluded that randomly polarized radiation is unnecessary and the degree of polarization of giant pulses must be more rigorously defined. Potential applications of the four-dimensional statistics of polarized noise are proposed in § 5.

2. POLARIZATION ALGEBRA

This section reviews the relevant algebra of both Jones and Mueller representations of polarimetric transformations. Unless otherwise noted, the notation and terminology synthesizes that of the similar approaches to polarization algebra presented by Cloude (1986), Britton (2000), and Hamaker (2000).

2.1. Jones Calculus

The polarization of electromagnetic radiation is described by the second-order statistics of the transverse electric field vector, \mathbf{e} , as represented by the complex 2×2 coherency matrix, $\boldsymbol{\rho} \equiv \langle \mathbf{e} \mathbf{e}^\dagger \rangle$ (Born & Wolf 1980). Here, the angular brackets denote an ensemble average, \mathbf{e}^\dagger is the Hermitian transpose of \mathbf{e} , and an outer product is implied by the treatment of \mathbf{e} as a column vector. A useful geometric relationship between the complex two-dimensional space of the coherency matrix and the real four-dimensional space of the Stokes parameters is expressed by the following pair of equations:

$$\boldsymbol{\rho} = S_k \boldsymbol{\sigma}_k / 2 \quad (1)$$

$$S_k = \text{Tr}(\boldsymbol{\sigma}_k \boldsymbol{\rho}). \quad (2)$$

Here, S_k are the four Stokes parameters, Einstein notation is used to imply a sum over repeated indices, $0 \leq k \leq 3$, $\boldsymbol{\sigma}_0$ is the 2×2 identity matrix, $\boldsymbol{\sigma}_{1-3}$ are the Pauli matrices, and Tr is the matrix trace operator. The Stokes four-vector is composed of the total intensity S_0 and the polarization vector, $\mathbf{S} = (S_1, S_2, S_3)$. Equation (1) expresses the coherency matrix as a linear combination of Hermitian basis matrices; equation (2) represents the Stokes parameters as the projections of

the coherency matrix onto the basis matrices. These properties are used to interpret the well-studied statistics of random matrices through the familiar Stokes parameters.

Linear transformations of the electric field vector are represented using complex 2×2 Jones matrices. Substitution of $\mathbf{e}' = \mathbf{J}\mathbf{e}$ into the definition of the coherency matrix yields the congruence transformation,

$$\boldsymbol{\rho}' = \mathbf{J}\boldsymbol{\rho}\mathbf{J}^\dagger, \quad (3)$$

which forms the basis of the various coordinate transformations that are exploited throughout this work. If \mathbf{J} is non-singular, it can be decomposed into the product of a Hermitian matrix and a unitary matrix known as its polar decomposition,

$$\mathbf{J} = J \mathbf{B}_{\hat{\mathbf{m}}}(\beta) \mathbf{R}_{\hat{\mathbf{n}}}(\phi), \quad (4)$$

where $J = |\mathbf{J}|^{1/2}$, $\mathbf{B}_{\hat{\mathbf{m}}}(\beta)$ is positive-definite Hermitian, and $\mathbf{R}_{\hat{\mathbf{n}}}(\phi)$ is unitary; both $\mathbf{B}_{\hat{\mathbf{m}}}(\beta)$ and $\mathbf{R}_{\hat{\mathbf{n}}}(\phi)$ are unimodular. Under the congruence transformation of the coherency matrix, the Hermitian matrix

$$\mathbf{B}_{\hat{\mathbf{m}}}(\beta) = \exp(\beta \hat{\mathbf{m}} \cdot \boldsymbol{\sigma}) = \sigma_0 \cosh \beta + \hat{\mathbf{m}} \cdot \boldsymbol{\sigma} \sinh \beta \quad (5)$$

effects a Lorentz boost of the Stokes four-vector along the $\hat{\mathbf{m}}$ axis by a hyperbolic angle 2β . As the Lorentz transformation of a spacetime event mixes temporal and spatial dimensions, the polarimetric boost mixes total and polarized intensities, thereby altering the degree of polarization. In contrast, the unitary matrix

$$\mathbf{R}_{\hat{\mathbf{n}}}(\phi) = \exp(i\phi \hat{\mathbf{n}} \cdot \boldsymbol{\sigma}) = \sigma_0 \cos \phi + i\hat{\mathbf{n}} \cdot \boldsymbol{\sigma} \sin \phi \quad (6)$$

rotates the Stokes polarization vector about the $\hat{\mathbf{n}}$ axis by an angle 2ϕ . As the orthogonal transformation of a vector in Euclidean space preserves its length, the polarimetric rotation leaves the degree of polarization unchanged.

These geometric interpretations promote a more intuitive treatment of the matrix equations that typically arise in polarimetry. Boost transformations can be utilized to convert unpolarized radiation into partially polarized radiation, and rotation transformations can be used to choose the orthonormal basis that maximizes symmetry. These properties are exploited in § 3 to simplify the relevant mathematical expressions that describe the four-dimensional joint distribution of the Stokes parameters.

2.2. Eigen Decomposition

It proves useful in § 3 to express the coherency matrix as a similarity transformation known as its eigen decomposition,

$$\boldsymbol{\rho} = \mathbf{R} \begin{pmatrix} \lambda_0 & 0 \\ 0 & \lambda_1 \end{pmatrix} \mathbf{R}^{-1}. \quad (7)$$

Here, $\mathbf{R} = (\mathbf{e}_0 \mathbf{e}_1)$ is a 2×2 matrix with columns equal to the eigenvectors of $\boldsymbol{\rho}$, and λ_m are the corresponding eigenvalues, given by $\lambda = (S_0 \pm |\mathbf{S}|)/2 = (1 \pm P)S_0/2$, where $P = S_0/|\mathbf{S}|$ is the degree of polarization. If the signal is completely polarized, then $\lambda_1 = 0$. If the signal is unpolarized, then there is a single 2-fold degenerate eigenvalue, $\lambda = S_0/2$ and \mathbf{R} is undefined.

If the eigenvectors are normalized such that $\mathbf{e}_k^\dagger \mathbf{e}_k = 1$, then equation (7) is equivalent to a congruence transformation by the unitary matrix, \mathbf{R} . In the natural basis defined by \mathbf{R}^\dagger , the eigenvalues λ_m are equal to the variances of two uncorrelated signals received by orthogonally polarized receptors described by the eigenvectors. The total intensity, $S_0 = \lambda_0 + \lambda_1$; the polarized intensity, $S_1 = |\mathbf{S}| = \lambda_0 - \lambda_1$; and $S_2 = S_3 = 0$. That is, \mathbf{R}^\dagger rotates the basis such that the mean polarization vector points along S_1 , providing cylindrical symmetry about this axis.

2.3. Mueller Calculus

The congruence transformation of the coherency matrix by any Jones matrix \mathbf{J} may be represented by an equivalent linear transformation of the Stokes parameters by a real-valued 4×4 Mueller matrix

$$M_i^k = \frac{1}{2} \text{Tr}(\boldsymbol{\sigma}_i \mathbf{J} \boldsymbol{\sigma}_k \mathbf{J}^\dagger), \quad (8)$$

such that

$$S'_i = M_i^k S_k. \quad (9)$$

Mueller matrices that have an equivalent Jones matrix are called pure, and such transformations are related to the Lorentz group (e.g. Barakat 1963; Britton 2000). This motivates the definition of an inner product

$$\langle A, B \rangle \equiv A^k B_k = \eta^{kk} A_k B_k = A_0 B_0 - \mathbf{A} \cdot \mathbf{B}, \quad (10)$$

where A and B are Stokes four-vectors and η_{ij} is the Minkowski metric tensor with signature $(+, -, -, -)$. The Lorentz invariant of a Stokes four-vector is equal to four times the determinant of the coherency matrix; that is,

$$S^2 \equiv \langle S, S \rangle = S_0^2 - |\mathbf{S}|^2 = 4|\boldsymbol{\rho}| \quad (11)$$

Similarly, the Euclidean norm $\|S\|$ is twice the Frobenius norm of the coherency matrix $\|\boldsymbol{\rho}\|$; i.e.

$$\|S\|^2 \equiv S_0^2 + |\mathbf{S}|^2 = 4\|\boldsymbol{\rho}\|^2. \quad (12)$$

The coherency matrix is a positive semi-definite Hermitian matrix; therefore, the Lorentz invariant of any physically realizable source of radiation is greater than or equal to zero. It is equal to zero only for completely polarized radiation, when the degree of polarization is unity ($S_0 = |\mathbf{S}|$). As with the spacetime null interval, no linear transformation of the electric field can alter the degree of polarization of a completely polarized source.

3. JOINT DISTRIBUTION FUNCTION

In this section, the joint distribution functions of the Stokes parameters for a stationary stochastic source of polarized radiation are derived. Three regimes of interest are considered: single samples, local means, and ensemble averages of large numbers of samples. The electric field vector is assumed to have a jointly normal density function as described by [Goodman \(1963\)](#). This distribution may not accurately describe the possibly non-linear electric field of intense non-thermal radiation. For example, over a limited range of pulse phase, the fluctuations in the intensity of the Vela pulsar have a lognormal distribution that is consistent with the predictions of stochastic growth theory ([Cairns et al. 2001](#)). The normal distribution is a valid choice if the pulsar signal can be accurately modeled as polarized shot-noise, provided that the density of shots is sufficiently high ([Cordes 1976](#)). It is also the minimal assumption if no information about the higher-order moments of the field is available.

3.1. Single Samples

As second-order moments of the electric field, the coherency matrix and Stokes parameters are defined only after an average is made over some number of samples. Given a single instance of the electric field \mathbf{e} (for example, discretely sampled at an infinitesimal moment in time) define the instantaneous coherency matrix, $\mathbf{r} = \mathbf{e} \mathbf{e}^\dagger$, and Stokes parameters, $s_k = \text{Tr}(\boldsymbol{\sigma}_k \mathbf{r})$, such that the ensemble averages, $\boldsymbol{\rho} = \langle \mathbf{r} \rangle$ and $S_k = \langle s_k \rangle$. It is trivial to show that the determinant of the instantaneous coherency matrix, $|\mathbf{r}| = 0$, regardless of the degree of polarization of the source or the probability density of the electric field. That is, the instantaneous degree of polarization is undefined.

The complex-valued components of \mathbf{e} are the analytic signals associated with the real-valued voltages measured in each receptor. If the voltages are normally distributed with zero mean, then \mathbf{e} has a bivariate complex normal distribution ([Goodman 1963](#)),

$$f(\mathbf{e}) = \frac{1}{\pi^2 |\boldsymbol{\rho}|} \exp(-\mathbf{e}^\dagger \boldsymbol{\rho}^{-1} \mathbf{e}), \quad (13)$$

where $\boldsymbol{\rho} = S_k \boldsymbol{\sigma}_k / 2$ is the population mean coherency matrix. To compute the probability density function of the instantaneous Stokes parameters, note that $f(\mathbf{e})$ is independent of the absolute phase of \mathbf{e} . Conversion to polar coordinates and marginalization over this variable yields the intermediate result,

$$f(|e_0|, |e_1|, \psi) = \frac{2|e_0||e_1|}{\pi |\boldsymbol{\rho}|} \exp(-\mathbf{e}^\dagger \boldsymbol{\rho}^{-1} \mathbf{e}), \quad (14)$$

where ψ is the instantaneous phase difference between e_0 and e_1 . This result may be compared with equation

(2.10) of [Barakat \(1987\)](#), except that here the evaluation of the inner product has been postponed. The three remaining degrees of freedom are described by the instantaneous polarization vector \mathbf{s} , for which the Jacobian determinant is

$$J(\mathbf{s}; |e_0|, |e_1|, \psi) = \left| \frac{\partial \mathbf{s}}{\partial (|e_0|, |e_1|, \psi)} \right| = 8|e_0||e_1||\mathbf{s}|. \quad (15)$$

Application of the above with

$$\boldsymbol{\rho}^{-1} = \frac{1}{2|\boldsymbol{\rho}|} (S_0 \boldsymbol{\sigma}_0 - \mathbf{S} \cdot \boldsymbol{\sigma}) = \frac{2}{S^2} S^k \boldsymbol{\sigma}_k \quad (16)$$

and

$$\mathbf{e}^\dagger \boldsymbol{\rho}^{-1} \mathbf{e} = \text{Tr}(\mathbf{e}^\dagger \boldsymbol{\rho}^{-1} \mathbf{e}) = \text{Tr}(\boldsymbol{\rho}^{-1} \mathbf{r}) \quad (17)$$

yields the four-dimensional joint distribution of the instantaneous Stokes parameters,

$$f(\mathbf{s}) = \frac{\delta(s_0 - |\mathbf{S}|)}{\pi S^2 s_0} \exp\left(-\frac{2\langle \mathbf{S}, \mathbf{s} \rangle}{S^2}\right), \quad (18)$$

where δ is the Dirac delta function and s_0 is the instantaneous total intensity. This result is consistent with equation (11) of [Eliyah \(1994\)](#). Converting to spherical polar coordinates, the inner product $\langle \mathbf{S}, \mathbf{s} \rangle = s_0(S_0 - |\mathbf{S}|) \cos \theta$, where θ is the angle between \mathbf{s} and \mathbf{S} . Subsequent integration over \mathbf{s} yields the marginal distribution of the instantaneous total intensity,

$$f(s_0) = \frac{2}{|\mathbf{S}|} \exp\left(-\frac{2s_0 S_0}{S^2}\right) \sinh\left(\frac{2s_0 |\mathbf{S}|}{S^2}\right), \quad (19)$$

which has mean S_0 and variance $\|\mathbf{S}\|^2/2$. This distribution is consistent with equation (13) of [Mandel \(1963\)](#) and equation (4) of [Fercher & Steeger \(1981\)](#). As noted by these authors, the total intensity becomes χ^2 distributed in the two cases of unpolarized and completely polarized radiation. This is easily seen in the natural basis defined by the eigen decomposition of the coherency matrix. As the squared norm of a complex number, the instantaneous intensity in each of the two orthogonally polarized modes is χ^2 distributed with two degrees of freedom. If the signal is unpolarized, then each mode contributes identically and the total intensity is χ^2 distributed with four degrees of freedom. If the signal is 100% polarized, then only one mode contributes and the total intensity is χ^2 distributed with two degrees of freedom.

The marginal distributions of the instantaneous Stokes polarization vector components are most easily derived in the natural basis, where $\langle \mathbf{S}, \mathbf{s} \rangle = s_0 S_0 - s_1 S_1$. Converting \mathbf{s} to cylindrical coordinates with the axis of symmetry along S_1 then integrating equation (18) over the radial and azimuthal dimensions (as well as the total intensity) yields the marginal distribution of the instantaneous major polarization,

$$f(s_1) = \frac{1}{S_0} \exp\left(-\frac{2|s_1| S_0}{S^2}\right) \exp\left(\frac{2s_1 |\mathbf{S}|}{S^2}\right). \quad (20)$$

This is an asymmetric Laplace density with mean S_1 and variance $\|S\|^2/2$, consistent with equation (8) of [Fercher & Steeger \(1981\)](#). The marginal distribution of the instantaneous minor polarization s_2 is derived in Appendix A; by symmetry, equation (A4) yields

$$f(s_{2,3}) = \frac{1}{S} \exp\left(-\frac{2|s_{2,3}|}{S}\right), \quad (21)$$

where S is the Lorentz interval. This is a symmetric Laplace density with mean zero and variance $S^2/2$, as in equation (16) of [Fercher & Steeger \(1981\)](#).

Equations (19) through (21) are plotted in Figure 1. The bottom two panels illustrate the asymmetric, three-dimensional Laplace distribution of the instantaneous polarization vector \mathbf{s} ; the top panel shows the distribution of the magnitude of this vector $s_0 = |\mathbf{s}|$. Qualitatively, instances of \mathbf{s} are distributed as a tapered needle that points along the major polarization axis, with the greatest density of instances in the head of the needle at the origin. For unpolarized radiation, the distribution is spherically symmetric and $f(s_1) = f(s_{2,3})$. For completely polarized radiation, $f(s_{2,3}) = \delta(s_{2,3})$ and $s_1 = s_0$; that is, the distribution of \mathbf{s} becomes one-dimensional and exponentially distributed along the positive S_1 axis.

3.2. Local Means

The distribution of the local mean of $n > 1$ independent and identically distributed instances of the Stokes parameters $\hat{\mathbf{s}}$ are derived from the distribution of the local mean coherency matrix

$$\hat{\boldsymbol{\rho}} = \frac{1}{n} \sum_{i=1}^n \mathbf{e}_i \mathbf{e}_i^\dagger = \frac{1}{2} \hat{\mathbf{s}}_k \boldsymbol{\sigma}_k, \quad (22)$$

which has a complex Wishart distribution with n degrees of freedom ([Wishart 1928](#); [Goodman 1963](#); [Touzi & Lopes 1996](#)); i.e.

$$f(\hat{\boldsymbol{\rho}}) = \frac{n^{2n} |\hat{\boldsymbol{\rho}}|^{n-2}}{\pi \Gamma(n) \Gamma(n-1) |\boldsymbol{\rho}|^n} \exp(-n \text{Tr}[\boldsymbol{\rho}^{-1} \hat{\boldsymbol{\rho}}]). \quad (23)$$

The Wishart distribution is a multivariate generalization of the χ^2 distribution, and plays an important role in communications engineering and information theory. As in § 3.1, the Jacobian determinant

$$J(S_k, \boldsymbol{\rho}) = \left| \frac{\partial S_k}{\partial \boldsymbol{\rho}} \right| = 8 \quad (24)$$

and equation (16) are used to arrive at the joint distribution function of the local mean Stokes parameters,

$$f(\hat{\mathbf{s}}) = \frac{2n^{2n} \hat{\mathbf{s}}^{2(n-2)}}{\pi \Gamma(n) \Gamma(n-1) S^{2n}} \exp\left(-\frac{2n \langle S, \hat{\mathbf{s}} \rangle}{S^2}\right). \quad (25)$$

In Appendix B, this joint distribution is used to derive the probability density and the first two moments of

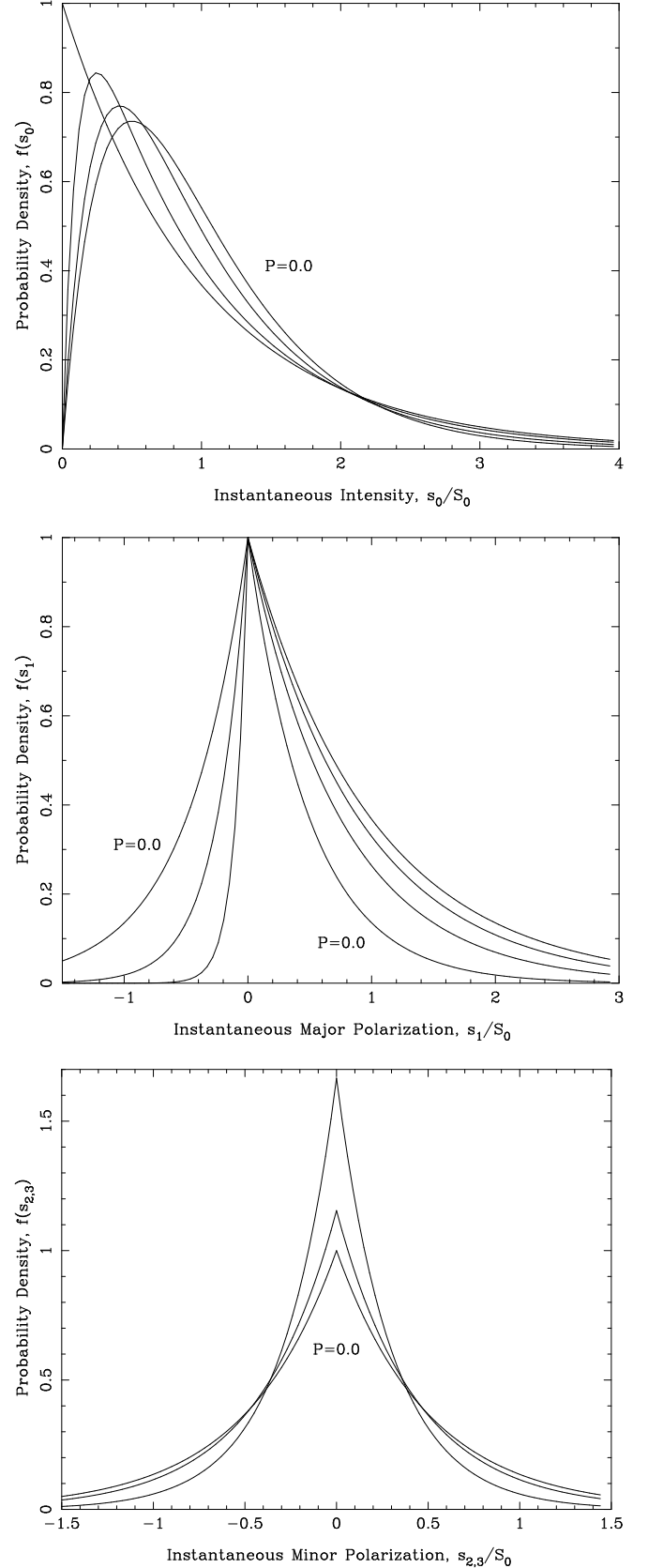


Figure 1. Probability densities of the instantaneous Stokes parameters as a function of the degree of polarization, P . From top to bottom are the density functions of the total intensity, the major polarization, and the minor polarizations. In each panel, the unpolarized case is labeled $P = 0$ then followed by $P = 0.5$, $P = 0.8$ and, where applicable, $P = 1.0$.

the local mean degree of polarization, $p = |\hat{s}|/\hat{s}_0$. In Figure 2, the distribution of p is plotted as a function of the intrinsic degree of polarization P and the number of degrees of freedom n . Note that, when $P = 1$, $f(p) = \delta(p - 1)$; therefore, this case is not shown. The expected value of p as a function P and n is plotted in Figure 3; the standard deviation σ_p is similarly plotted in Figure 4.

Figure 3 demonstrates that the self noise intrinsic to a stationary stochastic source of polarized radiation induces a bias, $\langle p \rangle - P$, in the estimated degree of polarization. The bias and standard deviation define the minimum sample size required to estimate the degree of polarization to a certain level of accuracy and precision. Given the sample size and a measurement of p , the probability density of p (eqs. [B6] and [B7]) or the expectation value of p (eq. [B8]) could be used to numerically estimate the intrinsic degree of polarization using methods similar to those reviewed by Simmons & Stewart (1985).

3.3. Ensemble Averages

By the central limit theorem, at large n the mean Stokes parameters tend toward a multivariate normal distribution

$$f(\bar{S}) = \frac{1}{4\pi^2 |\mathbf{C}|^{1/2}} \exp\left(-\frac{1}{2} \Delta S^T \mathbf{C}^{-1} \Delta S\right), \quad (26)$$

where $\Delta S = \bar{S} - S$ and \mathbf{C} is the covariance matrix of the Stokes parameters. To derive the components of \mathbf{C} , consider a completely unpolarized, dimensionless signal with unit intensity (that is, with mean coherency matrix $\rho_u = \sigma_0/2$ and mean Stokes parameters $S_u = [1, 0, 0, 0]$) and covariance matrix $\mathbf{C}_u = \zeta^2 \mathbf{I}$, where ζ^2 is the dimensionless variance of each Stokes parameter and \mathbf{I} is the 4×4 identity matrix. This unpolarized signal may be transformed into any partially polarized signal with mean coherency matrix ρ via a congruence transformation

$$\rho = \mathbf{b} \rho_u \mathbf{b}^\dagger = \mathbf{b} \mathbf{b}^\dagger / 2 = \mathbf{b}^2 / 2, \quad (27)$$

where \mathbf{b} is the Hermitian square root of 2ρ (e.g. Hamaker 2000) and the elements of ρ have physical dimensions such as flux density. The covariance matrix of the Stokes parameters of the resulting partially polarized signal is $\mathbf{C} = \mathbf{B} \mathbf{C}_u \mathbf{B}^T$, where \mathbf{B} is the Mueller matrix of \mathbf{b} , defined by equation (8). Noting that \mathbf{B} is symmetric, $\mathbf{C} = \zeta^2 \mathbf{B}^2$ is simply a scalar multiple of the Mueller matrix of ρ ; i.e.

$$C_{ij} = \zeta^2 (2S_i S_j - \eta_{ij} S^2). \quad (28)$$

This result is a generalization of equation (9) in Brosseau & Barakat (1992), which derives from the complex Gaussian moment theorem. In contrast, equation (28) requires no assumptions about the distribution of the electric field.

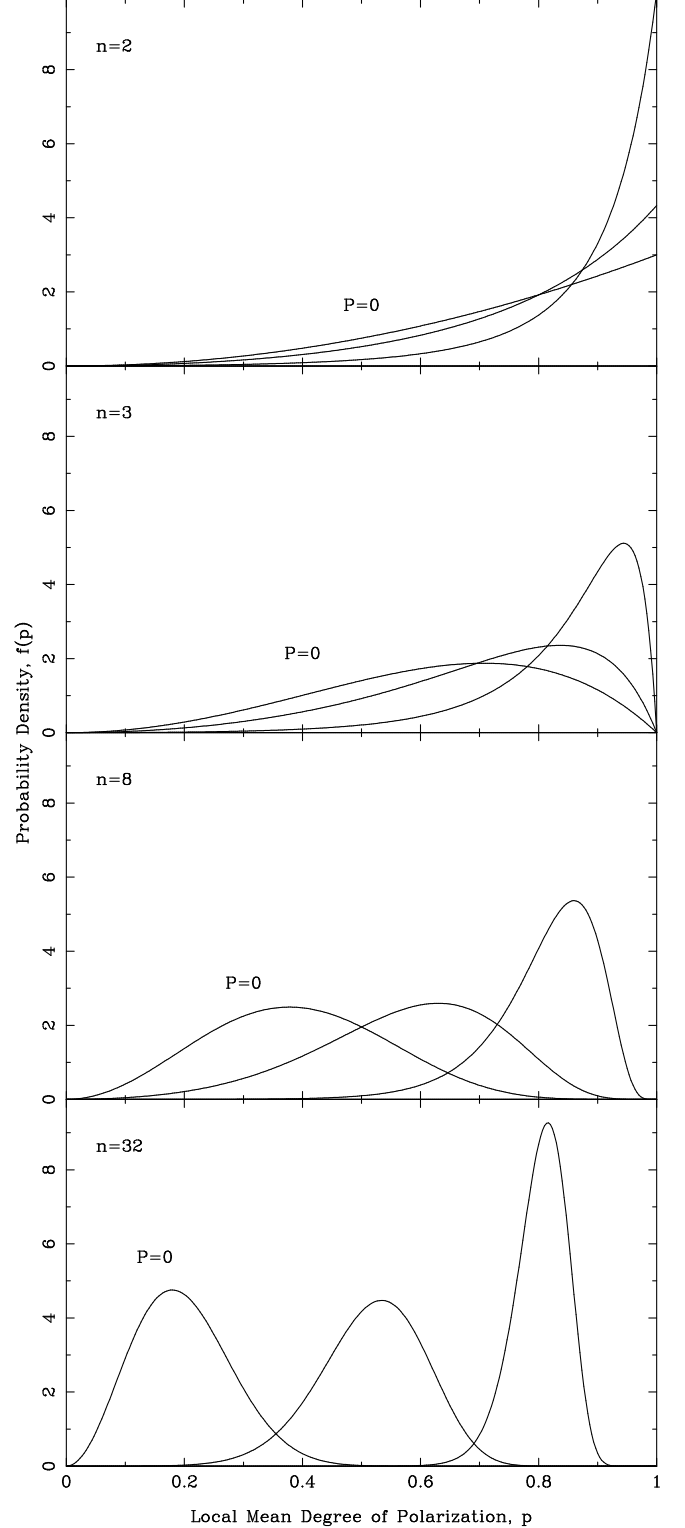


Figure 2. Probability densities of the local degree of polarization as function of the intrinsic degree of polarization, P , and the number of degrees of freedom, n . In each panel, the unpolarized case is labeled $P = 0$ then followed by $P = 0.5$ and $P = 0.8$.

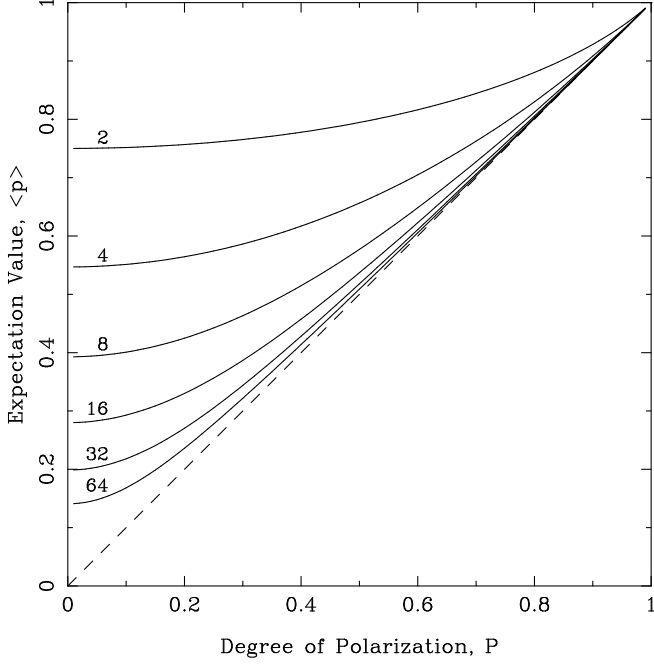


Figure 3. Expectation value of the local degree of polarization as a function of the intrinsic degree of polarization. The number of degrees of freedom is printed above each curve and the dashed line indicates $\langle p \rangle = P$.

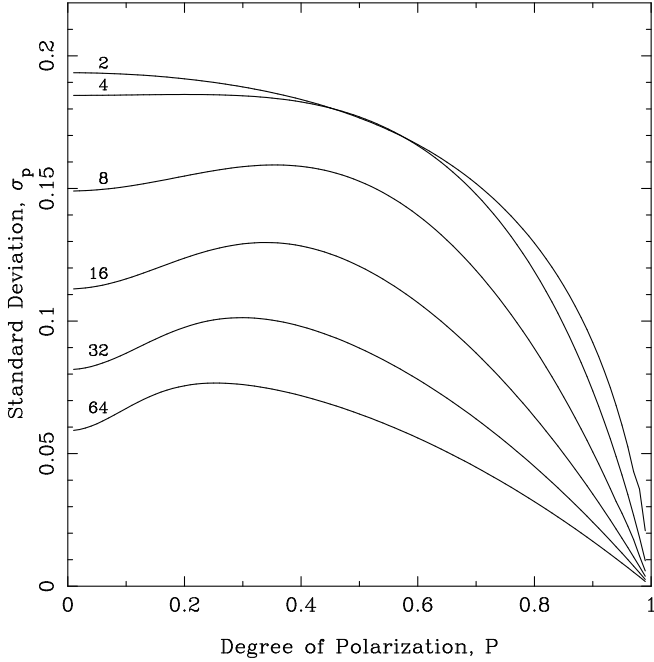


Figure 4. Standard deviation of the local degree of polarization as a function of the intrinsic degree of polarization. The number of degrees of freedom is printed above each curve.

The covariance matrix of the Stokes parameters has its simplest form in the natural basis defined by the eigen

decomposition of the coherency matrix, where

$$\mathbf{C}' = \zeta^2 \begin{pmatrix} \|S\|^2 & 2S_0|S| & 0 & 0 \\ 2S_0|S| & \|S\|^2 & 0 & 0 \\ 0 & 0 & S^2 & 0 \\ 0 & 0 & 0 & S^2 \end{pmatrix}. \quad (29)$$

Comparison between the diagonal of \mathbf{C}' and the variances of the distributions derived in § 3.1 yields the relationship between the dimensionless variance and the number of degrees of freedom, $\zeta^2 = (2n)^{-1}$. In the natural basis, it is also readily observed that the polarization vector \bar{S} is normally distributed as a prolate spheroid with axial ratio, $\epsilon = ((1 + P^2)/(1 - P^2))^{1/2}$. The dimension of the major axis of the spheroid is equal to the standard deviation of the total intensity and the dimension of the minor axis goes to zero as the degree of polarization approaches unity. Furthermore, the multiple correlation between \bar{S}_0 and \bar{S} is

$$R = \frac{2P}{1 + P^2}. \quad (30)$$

The multiple correlation ranges from 0 for an unpolarized source to 1 for a completely polarized source. It characterizes the correlation between total and polarized intensities and expresses the fact that the stochastic Stokes parameters cannot be treated in isolation.

4. APPLICATION TO RADIO PULSAR ASTRONOMY

The previous section develops the four-dimensional statistics of the Stokes parameters intrinsic to a single, stationary source of stochastic electromagnetic radiation. To apply these results to radio pulsar polarimetry, it is necessary to consider various observed properties of pulsar signals, including amplitude modulation, wave coherence, and the superposition of signals from multiple sources, such as instrumental noise and orthogonally polarized modes. Emphasis is placed on the statistical degrees of freedom of the radiation; in particular, the effects of amplitude modulation and wave coherence on the *identically distributed* and *independent* conditions of the central limit theorem are considered. Attention is then focused on two areas of concern: randomly polarized radiation and giant pulse polarimetry.

4.1. Amplitude Modulation

Radio pulsar signals are well described as amplitude-modulated noise (Rickett 1975). The modulation index is generally defined as $\beta = \sigma_0/S_0$, where σ_0 and S_0 are the standard deviation and mean of the total intensity. In single-pulse observations of radio pulsars, σ_0 is typically corrected for the instrumental noise estimated from the off-pulse baseline and the self noise is assumed to be

negligible. A value of β greater than zero is then interpreted as evidence of amplitude modulation. However, for intense sources of radiation, the self noise of the ensemble average total intensity, $\sigma_0 = \varsigma \|S\|$ (cf. eq. [29] of Cordes 1976) must be taken into account. That is, the self noise of the source induces a positive bias in the modulation index.

Amplitude modulation modifies the statistics of all four Stokes parameters. For example, under scalar amplitude modulation, the covariance matrix of the Stokes parameters becomes $\langle A^2 \rangle \mathbf{C}$, where A is the instantaneous intensity of the modulating function and $\langle A^2 \rangle \geq \langle A \rangle^2 = 1$. That is, amplitude modulation uniformly increases the covariances of the Stokes parameters. This can be interpreted as a reduction in the statistical degrees of freedom of the signal, which becomes dominated by the fraction of realizations that occur when $A \gg 1$. That is, especially when the modulations are deep, the samples are not identically distributed and the central limit theorem does not trivially apply.

4.2. Wave Coherence

The degrees of freedom of a stochastic process are also reduced when the samples are not independent. For plane-propagating electromagnetic radiation, statistical dependence is manifest in various forms of wave coherence, including that between the orthogonal components of the wave vector (i.e. polarization) and that between instances of the field at different coordinates (e.g. spectral, spatial, temporal). In radio pulsar observations, wave coherence properties may be modified by propagation in the pulsar magnetosphere and the interstellar medium (e.g. Lyutikov & Parikh 2000; Melrose & Macquart 1998; Macquart & Melrose 2000).

Given the coherence time τ_c (Mandel 1958, 1959) of a band-limited source of Gaussian noise, the effective number of degrees of freedom is

$$N_{\text{eff}} = \frac{T}{\tau_c + \tau} \leq \frac{T}{\tau} = n, \quad (31)$$

where T is the integration interval, τ is the sampling interval, and n is the number of discrete time samples in the interval T . That is, owing to wave coherence, the signal could be encoded by N_{eff} independent samples without any loss of information.

Substituting $n = N_{\text{eff}}$ into equation (25) or $\varsigma^2 \propto 1/N_{\text{eff}}$ into equation (26), it is seen that wave coherence inflates the four-dimensional volume occupied by the joint distribution of the mean Stokes parameters. With respect to the statistics of independent samples, this inflation increases both the modulation index of the mean total intensity and the eigenvalues of the covariance matrix of the mean Stokes polarization vector (Edwards & Stappers 2004; McKinnon 2004). Referring

to Figure 3, it is readily observed that wave coherence also increases the local mean degree of polarization.

If only the covariance matrix of the Stokes parameters is measured, the effects of wave coherence are indistinguishable from those of amplitude modulation. In fact, the non-stationary statistics that arise from amplitude modulation can be described by their spectral coherence properties (e.g. Bertolotti et al. 1995). The various types of wave coherence may be differentiated via auto-correlation and fluctuation spectral estimates (e.g. Cordes 1976; Edwards & Stappers 2003, 2004; Jenet & Gil 2004) that are outside the scope of the current treatment.

4.3. Incoherent Sum

When one or more incoherent sources of radiation are added together, the resulting covariance matrix of the total ensemble mean Stokes parameters is the sum of the covariance matrices of the individual sources. For example, unpolarized noise adds a term to the diagonal of the covariance matrix, such that

$$C'_{ij} = C_{ij} + \delta_{ij} \xi^2,$$

thereby reducing both the ellipticity of the distribution of the polarization vector and the multiple correlation between total and polarized intensities.

The incoherent addition of signals with different polarizations, especially the superposition of orthogonally polarized modes, also decreases the degree of polarization of the mean Stokes parameters. If the modes are covariant (e.g. McKinnon & Stinebring 1998), then the covariance matrix of the sum includes cross-covariance terms. For example, consider the incoherent sum of two sources described by Stokes parameters A and B . If the intensities of the two modes are correlated, then the resulting covariance matrix is given by

$$\mathbf{C} = \mathbf{C}_A + \mathbf{C}_B + \mathbf{\Xi} + \mathbf{\Xi}^T, \quad (32)$$

where \mathbf{C}_A and \mathbf{C}_B are defined as in equation (28) and the cross-covariance matrix is

$$\Xi_{ij} = \varrho \varsigma_A \varsigma_B A_i B_j, \quad (33)$$

where ϱ is the intensity correlation coefficient. As shown in Appendix C, the incoherent superposition of covariant orthogonally polarized modes causes the variance of the total intensity to increase while that of the major polarization decreases. (The major polarization is defined by the eigen decomposition and is parallel to the major axis of the spheroidal distribution of \mathbf{S} .) Furthermore, it is shown that the four-dimensional covariance matrix of the Stokes parameters can be used to derive the correlation coefficient as well as the intensities and degrees of polarization of superposed covariant orthogonal modes.

4.4. Randomly Polarized Radiation

McKinnon (2004) and Edwards & Stappers (2004) independently developed and applied novel eigenvalue analyses of the three-dimensional covariance matrix of the Stokes polarization vector \mathbf{S} . Each noted an apparent excess dispersion of \mathbf{S} and concluded that it is due to the incoherent addition of randomly polarized radiation intrinsic to the pulsar signal. This hypothesis is based on the assumption that, apart from the proposed randomly polarized component, the noise in each of the Stokes parameters is purely instrumental, a premise that breaks down for sources as bright as the pulsars studied in these experiments.

For example, McKinnon (2004) analyzed observations of PSRs B2020+28 and B1929+10 that were recorded with the Arecibo 300 m antenna when the forward gain was 8 K/Jy and the system temperature was 40 K (Stinebring et al. 1984). Referring to the average pulse profiles presented in Figure 2 of McKinnon (2004), the total intensity of PSR B2020+28 peaks at 8 Jy where the modulation index is ~ 1.3 . That is, the noise intrinsic to the pulsar signal exceeds the system equivalent flux density (SEFD; ~ 5 Jy) by as much as 100% (cf. Figure 6 of McKinnon & Stinebring 2000). Similarly, the self noise of PSR B1929+10 is as much as 50% of the SEFD. In both cases, source-intrinsic noise statistics cannot be neglected. To quantify the impact of self noise on single pulse polarimetry, the results of McKinnon (2004) are revisited. Note that Edwards & Stappers (2004) focused on the non-orthogonal modes of PSR B0329+54 and reported neither the instrumental sensitivity nor the statistics of the total intensity; therefore, this experiment is not reviewed here.

Figures 3 and 4 of McKinnon (2004) present two-dimensional projections of the ellipsoidal distributions of \mathbf{S} at different pulse phases, along with the dimensions of the major axis a_1 and minor axes, a_2 and a_3 , at each phase. Panel a) in each of these plots indicates the off-pulse, instrumental noise σ_n in each component of the Stokes polarization vector; for PSR B2020+28, $\sigma_n \simeq 0.1$ Jy and, for PSR B1929+10, $\sigma_n \simeq 0.04$ Jy. Figures 2-4 are summarized in Table 1, which lists the pulse phase bin number; the modulation index β ; the total intensity S_0 ; and the standard deviations of the total intensity $\sigma_0 = \beta S_0 + \sigma_n$, the major polarization $\sigma_1 = a_1$, and the minor polarizations $\sigma_\perp = a_2 \simeq a_3$.

As shown in § 3.3, the standard deviation of the total intensity and the major axis of the spheroidal distribution of the polarization vector should be equal; however, for every phase bin listed in Table 1, $\sigma_0 > \sigma_1$. That is, there is no excess dispersion of the polarization vector and therefore no need for additional randomly polarized radiation; rather, the excess dispersion of the total

intensity requires explanation. Noting that scalar amplitude modulation and wave coherence uniformly inflate the covariance matrix of the Stokes parameters, one possible explanation for $\sigma_0 > \sigma_1$ is the incoherent superposition of covariant orthogonally polarized modes (see Appendix C). The coefficient of correlation between the mode intensities ϱ in equations (C10) and (C11) is equivalent to r_{12} in the analogous equations (5) and (6) of McKinnon & Stinebring (1998). The last term in all four of these equations indicates that positive correlation between the mode intensities increases the variance of the total intensity ($\sigma_0^2 = C_{00} + \sigma_n^2$) and decreases that of the major polarization ($\sigma_1^2 = C_{11} + \sigma_n^2$). (Anti-correlated mode intensities have the opposite effect.) The increased variance of the total intensity also explains why orthogonally polarized modes typically coincide with increased amplitude modulation (McKinnon 2004).

Similarly, equation (C12) shows that the self noise of partially polarized modes increases the dimensions of the minor axes ($a_2^2 = C_{22} + \sigma_n^2$ and $a_3^2 = C_{33} + \sigma_n^2$). The source-intrinsic contribution diminishes to zero only for 100% polarized modes. For all of the phase bins listed in Table 1, $\sigma_\perp > \sigma_n$, indicating that the modes are not completely polarized, as has been previously assumed (McKinnon & Stinebring 1998; McKinnon & Stinebring 2000).

Equations (C10) to (C13) and the discussion in Appendix C motivate the development of a new technique for producing mode-separated profiles. From the four-dimensional covariance matrix of the Stokes parameters, it is possible to derive the mode intensity correlation coefficient as well as the intensities and degrees of polarization of the modes. These values and the mean Stokes parameters, computed as a function of pulse phase, can be used to decompose the pulse profile into the separate contributions of the orthogonal modes.

4.5. Giant Pulses

The estimation of the degree of polarization of giant pulses is beset by fundamental limitations. On one hand, giant pulses remain unresolved at the highest time resolutions achieved to date. On the other hand, a sufficiently large number of independent samples must be averaged before an accurate estimate of polarization is possible. Even if many time samples are averaged, those samples may be correlated due to scattering on inhomogeneities in the interstellar medium and/or the mean may be dominated by a single unresolved giant nanopulse that greatly reduces the effective degrees of freedom.

For example, Popov et al. (2006) presented a histogram of the degree of circular polarization of giant pulses from the Crab pulsar observed at 600 MHz. The histogram is interpreted as evidence that each giant

Table 1. Eigenvalue Analysis from [McKinnon \(2004\)](#)

| Bin | β | S_0 (Jy) | σ_0 | σ_1 | σ_\perp |
|--------------|---------|------------|------------|------------|----------------|
| PSR B2020+28 | | | | | |
| 61 | 0.45 | 5.5 | 2.58 | 1.14 | 0.59 |
| 74 | 0.19 | 2.8 | 0.63 | 0.33 | 0.30 |
| 91 | 0.56 | 3.1 | 1.84 | 0.91 | 0.71 |
| PSR B1929+10 | | | | | |
| 90 | 0.55 | 0.68 | 0.41 | 0.32 | 0.09 |
| 119 | 0.68 | 1.35 | 0.96 | 0.63 | 0.13 |
| 125 | 0.65 | 1.00 | 0.69 | 0.46 | 0.10 |

pulse is the sum of ~ 100 nanopulses, each with 100% circular polarization. However, referring to Figure 4, the width of the distribution is also consistent with that of completely unpolarized radiation with $\lesssim 2$ degrees of freedom. Although the data were averaged over 256 samples to $32 \mu\text{s}$ resolution, the characteristic timescale of scattering in these observations was estimated to be $45 \pm 5 \mu\text{s}$; therefore, the effective number of degrees of freedom is of the order of unity.

Small-number statistics also limit the conclusions that can be drawn from the correlations between giant pulse spectra presented in Figure 12 of [Cordes et al. \(2004\)](#). The asymptotic correlation coefficient at small lag was interpreted as evidence that nanopulses are highly polarized. However, with only one estimate of the correlation coefficient at a lag less than 0.1 seconds, the extrapolation to nanosecond resolution is questionable. Therefore, the constraint on the degree of polarization at this timescale is of negligible significance.

5. CONCLUSION

A four-dimensional statistical description of polarization is presented that exploits the homomorphism between the Lorentz group and the transformation properties of the Stokes parameters. Within this framework, a generalized expression for the covariance matrix of the Stokes parameters is developed and applied to the analysis of single-pulse polarization. The consideration of source-intrinsic noise renders randomly polarized radiation unnecessary, explains the coincidence between increased amplitude modulation and orthogonal mode fluctuations, and indicates that orthogonally polarized modes are partially polarized. Furthermore, the four-

dimensional covariance matrix of the Stokes parameters enables estimation of the mode intensities, degrees of polarization, intensity correlation coefficient, and effective degrees of freedom of covariant orthogonally polarized modes. Measured as a function of pulse phase, these parameters may be used to produce mode-separated profiles without any assumptions about the intrinsic degree of mode polarization.

The formalism is also used to derive the first and second moments of the degree of polarization as a function of the intrinsic degree of polarization and the number of degrees of freedom of the stochastic process. These are used to demonstrate that giant pulse polarimetry is fundamentally limited by systematic bias due to insufficient statistical degrees of freedom. The discussions of amplitude modulation in § 4.1 and wave coherence in § 4.2 serve to illustrate the difficulties in defining an appropriate average when the central limit theorem cannot be trivially applied. In this regard, the approach employed in this paper is complimentary to previous analyses that make use of auto-correlation functions and fluctuation spectra to separately measure the statistics of the total and polarized intensities. Useful new results may be derived by extending the techniques employed in these works to include the cross-correlation terms that describe the statistical dependences between the Stokes parameters.

I am grateful to J.P. Macquart for fruitful discussions and K. Stovall for technical assistance with the computer algebra system. The insightful comments of the referee led to significant improvements to the manuscript. M. Bailes, R. Bhat, J. Verbiest and M. Walker also provided helpful feedback on the text.

APPENDIX

A. MARGINAL DISTRIBUTIONS OF THE MINOR STOKES PARAMETERS

Equations (19) and (20) could have been also derived by first expressing equation (14) in the natural basis. Here, it takes the simplified form,

$$f(|e_0|, |e_1|, \psi) = \frac{1}{2\pi} f_0(|e_0|) f_1(|e_1|), \quad (\text{A1})$$

where

$$f_m(|e_m|) = \frac{2|e_m|}{\lambda_m} \exp\left(\frac{-|e_m|^2}{\lambda_m}\right) \quad (\text{A2})$$

are Rayleigh distributions. Note that in the natural basis, $|e_0|$, $|e_1|$, and ψ are statistically independent and ψ is uniformly distributed. The distributions of $s_0 = |e_0| + |e_1|$ and $s_1 = |e_0| - |e_1|$ may then be obtained from the convolution and cross-correlation, respectively, of $f_0(|e_0|)$ and $f_1(|e_1|)$. Similarly, following [Fercher & Steeger \(1981\)](#), equation (A1) is used to compute the marginal distribution of $s_2 = 2|e_0||e_1|\cos\psi$. In the natural cylindrical coordinates defined in § 3.1, the distribution of the radial dimension $\Lambda = (s_2^2 + s_3^2)^{-1/2} = 2|e_0||e_1|$ is found by integrating equation (A1) over ψ , then transforming the integrand to yield the intermediate result

$$f(\Lambda) = \int_0^\infty f_0(|e_0|)f_1\left(\frac{\Lambda}{2|e_0|}\right)\frac{1}{2|e_0|}d|e_0| = \frac{\Lambda}{\lambda_0\lambda_1}K_0\left(\frac{\Lambda}{\sqrt{\lambda_0\lambda_1}}\right), \quad (\text{A3})$$

where K_0 is a modified Bessel function of the second kind. As the azimuthal dimension ψ is uniformly distributed, the probability density of $\cos\psi$ is

$$f(\cos\psi) = \frac{1}{\pi\sqrt{1-\cos^2\psi}}.$$

Combining with $f(\Lambda)$ and performing another integral transformation yields

$$f(s_2) = \int_0^1 f(\cos\psi)f\left(\frac{s_2}{\cos\psi}\right)\frac{1}{\cos\psi}d\cos\psi = \frac{1}{S}\exp\left(-\frac{2s_2}{S}\right) \quad (\text{A4})$$

for $s_2 > 0$, where S is the Lorentz interval. By symmetry, a similar result is found for $s_2 < 0$.

B. DISTRIBUTION AND MOMENTS OF THE LOCAL MEAN DEGREE OF POLARIZATION

Conversion of equation (25) to spherical coordinates and integration over all orientations of the polarization vector \hat{s} yields the joint distribution of the local mean total and polarized intensities,

$$f_n(\hat{s}_0, |\hat{s}|) = \frac{4n^{2n-1}|\hat{s}|\hat{s}^{2(n-2)}}{\Gamma(n)\Gamma(n-1)|\mathbf{S}|S^{2(n-1)}} \exp\left(-\frac{2n\hat{s}_0S_0}{S^2}\right) \sinh\left(\frac{2n|\hat{s}||\mathbf{S}|}{S^2}\right) \quad (\text{B5})$$

This joint density is defined on $0 \leq |\hat{s}| \leq \hat{s}_0$ and is used to derive the distribution of the local mean degree of polarization, $p = |\hat{s}|/\hat{s}_0$, as a function of the intrinsic degree of polarization $P = |\mathbf{S}|/S_0$ and the number of samples averaged n :

$$f(p) = \int_0^\infty \hat{s}_0 f_n(\hat{s}_0, p\hat{s}_0) d\hat{s}_0 = \frac{2\Gamma(2n-1)}{\Gamma(n-1)\Gamma(n)} \frac{(P^2-1)^n p(p^2-1)^{n-2} \left([1-Pp]^{1-2n} - [1+Pp]^{1-2n}\right)}{2^{2n-1}P}. \quad (\text{B6})$$

As $P \rightarrow 0$,

$$f(p) = \frac{2\Gamma(2n-1)}{\Gamma(n-1)\Gamma(n)} (-1)^n 2^{2-2n} (2n-1) p^2 (p^2-1)^{n-2}. \quad (\text{B7})$$

The distribution of the local mean degree of polarization is plotted in Figure 2; its first and second moments are

$$\langle p \rangle = \int_0^1 p f(p) dp = (1-P^2)^n \Gamma(n + \frac{1}{2}) {}_3\tilde{F}_2\left(2, n, n + \frac{1}{2}; \frac{3}{2}, n + 1; P^2\right) \quad (\text{B8})$$

and

$$\langle p^2 \rangle = \int_0^1 p^2 f(p) dp = \frac{3(1-P^2)^n}{1+2n} {}_3\tilde{F}_2\left(\frac{5}{2}, n, n + \frac{1}{2}; \frac{3}{2}, n + \frac{3}{2}; P^2\right), \quad (\text{B9})$$

where ${}_3\tilde{F}_2$ is a regularized generalized hypergeometric function ([Wolfeben 2007](#)). These moments are used to calculate the variance of the local mean degree of polarization $\sigma_p^2 = \langle p^2 \rangle - \langle p \rangle^2$. The theoretical values of $\langle p \rangle$ and σ_p are plotted as a function of n and P in Figures 3 and 4.

C. COVARIANT ORTHOGONAL PARTIALLY POLARIZED MODES

Following the discussion in § 4.3, the covariance matrix of orthogonally polarized modes with correlated intensities is derived by starting with equation (32), neglecting instrumental noise and considering only the self noise of the modes.

If the modes A and B are orthogonally polarized, then $\mathbf{A} \cdot \mathbf{B} = -|\mathbf{A}||\mathbf{B}|$; furthermore, if A is the dominant mode, then $|\mathbf{A}| > |\mathbf{B}|$ and in the natural basis defined by A , the six non-zero elements of the covariance matrix are

$$C_{00} = \varsigma_A^2 \|A\|^2 + \varsigma_B^2 \|B\|^2 + 2\varrho\varsigma_A\varsigma_B A_0 B_0 \quad (\text{C10})$$

$$C_{11} = \varsigma_A^2 \|A\|^2 + \varsigma_B^2 \|B\|^2 - 2\varrho\varsigma_A\varsigma_B |\mathbf{A}||\mathbf{B}| \quad (\text{C11})$$

$$C_{22} = C_{33} = \varsigma_A^2 A^2 + \varsigma_B^2 B^2 \quad (\text{C12})$$

$$C_{01} = C_{10} = 2\varsigma_A^2 A_0 |\mathbf{A}| - 2\varsigma_B^2 B_0 |\mathbf{B}| + \varrho\varsigma_A\varsigma_B (B_0 |\mathbf{A}| - A_0 |\mathbf{B}|). \quad (\text{C13})$$

Including $S_0 = A_0 + B_0$ and $|\mathbf{S}| = |\mathbf{A}| - |\mathbf{B}|$, there are a total of seven unknowns and six unique constraints. However, if it is assumed that the modes have similar degrees of freedom (i.e. $\varsigma_A \simeq \varsigma_B$), then the system can be solved numerically; e.g. using the Newton-Raphson method (Press et al. 1992). In McKinnon (2004), C_{01} is not measured; therefore, no derived parameter estimates are currently presented.

REFERENCES

- Backer, D. C., & Rankin, J. M. 1980, *ApJS*, 42, 143
 Barakat, R. 1963, *J. Opt. Soc. Am.*, 53, 317
 Barakat, R. 1987, *J. Opt. Soc. Am. A*, 4, 1256
 Bertolotti, M., Ferrari, A., & Sereda, L. 1995, *J. Opt. Soc. Am. B*, 12, 341
 Born, M., & Wolf, E. 1980, *Principles of optics: electromagnetic theory of propagation, interference and diffraction of light* (New York: Pergamon)
 Britton, M. C. 2000, *ApJ*, 532, 1240
 Brosseau, C., & Barakat, R. 1992, *Opt. Comm.*, 91, 408
 Cairns, I. H., Johnston, S., & Das, P. 2001, *ApJ*, 563, L65
 Cloude, S. 1986, *Optik*, 75, 26
 Cognard, I., Shrauner, J. A., Taylor, J. H., & Thorsett, S. E. 1996, *ApJ*, 457, L81
 Cordes, J. M. 1976, *ApJ*, 208, 944
 Cordes, J. M., Bhat, N. D. R., Hankins, T. H., McLaughlin, M. A., & Kern, J. 2004, *ApJ*, 612, 375
 Cordes, J. M., & Hankins, T. H. 1977, *ApJ*, 218, 484
 Edwards, R. T., & Stappers, B. W. 2003, *A&A*, 407, 273
 —. 2004, *A&A*, 421, 681
 Eliyahu, D. 1994, *Phys. Rev. E*, 50, 2381
 Fercher, A. F., & Steeger, P. F. 1981, *Optica Acta*, 28, 443
 Goodman, N. R. 1963, *Ann. of Math. Stat.*, 34, 152
 Hamaker, J. P. 2000, *A&AS*, 143, 515
 Hankins, T. H., Kern, J. S., Weatherall, J. C., & Eilek, J. A. 2003, *Nature*, 422, 141
 Heiles, C., Campbell, D. B., & Rankin, J. M. 1970, *Nature*, 226, 529
 Jenet, F. A., & Gil, J. 2004, *ApJ*, 602, L89
 Lyutikov, M., & Parikh, A. 2000, *ApJ*, 541, 1016
 Macquart, J.-P., & Melrose, D. B. 2000, 62, 4177
 Manchester, R. N., Taylor, J. H., & Huguenin, G. R. 1975, *ApJ*, 196, 83
 Mandel, L. 1958, *Proc. Phys. Soc.*, 72, 1037
 —. 1959, *Proc. Phys. Soc.*, 74, 233
 —. 1963, *Proc. Phys. Soc.*, 81, 1104
 McKinnon, M., & Stinebring, D. 1998, *ApJ*, 502, 883
 McKinnon, M. M. 2002, *ApJ*, 568, 302
 —. 2003a, *ApJ*, 590, 1026
 —. 2003b, *ApJS*, 148, 519
 —. 2004, *ApJ*, 606, 1154
 —. 2006, *ApJ*, 645, 551
 McKinnon, M. M., & Stinebring, D. R. 2000, *ApJ*, 529, 435
 Melrose, D. B., & Macquart, J.-P. 1998, *ApJ*, 505, 921
 Popov, M., Soglasnov, V., Kondrat'ev, V., et al. 2006, *Astronomy Letters*, 50, 55
 Press, W. H., Teukolsky, S. A., Vetterling, W. T., & Flannery, B. P. 1992, *Numerical Recipes: The Art of Scientific Computing*, 2nd edition (Cambridge: Cambridge University Press)
 Rickett, B. J. 1975, *ApJ*, 197, 185
 Simmons, J. F. L., & Stewart, B. G. 1985, *A&A*, 142, 100
 Steeger, P. F., Asakura, T., Zocha, K., & Fercher, A. F. 1984, *J. Opt. Soc. Am. A*, 1, 677
 Stinebring, D. R., Cordes, J. M., Rankin, J. M., Weisberg, J. M., & Boriakoff, V. 1984, *ApJS*, 55, 247
 Taylor, J. H., Huguenin, G. R., Hirsch, R. M., & Manchester, R. N. 1971, *Astrophys. Lett.*, 9, 205
 Touzi, R., & Lopes, A. 1996, I. E. E. E. *Trans. Geoscience and Remote Sensing*, 34, 519
 van Straten, W., & Tiburzi, C. 2017, *ApJ*, 835, 293
 Wishart, J. 1928, *Biometrika*, 20A, 32
 Wolleben, M. 2007, *ApJ*, 664, 349

APPENDIX

The following additional material was not submitted to The Astrophysical Journal and was not peer reviewed. It is provided as further information for the interested reader.

D. ERRORS IN THIS MANUSCRIPT

The following errors in the published manuscript and in its published Erratum have been discussed and addressed in van Straten & Tiburzi (2017).

1. In section 3.3, it is argued that Equation (28) is true regardless of the distribution of the electric field; however, it is true only in the case of jointly normally distributed electric field components. In general, the covariance matrix also depends on the Stokes cumulant as shown in Section 2.3 of van Straten & Tiburzi (2017).

2. In section 4.1, it is argued that amplitude modulation uniformly increases the covariances of the Stokes parameters (i.e. the covariance matrix is multiplied by a scalar greater than unity). In fact, as shown in Section 4.2 of [van Straten & Tiburzi \(2017\)](#), scalar amplitude modulation increases the variance of the total intensity more than it increases the variances of the other three Stokes parameters.
3. In Section 4.3, it is incorrectly asserted that the covariance matrix of an incoherent sum of sources of radiation is simply the sum of the covariance matrices that describe the individual sources. Section 4.1 of [van Straten & Tiburzi \(2017\)](#) presents the correct expression.

E. MARGINAL DISTRIBUTIONS

The marginal distributions of the Stokes parameters are computed in the natural basis, where the axis of symmetry in cylindrical or spherical coordinates is aligned with the major polarization, S_1 .

E.1. Equation (19): Instantaneous Intensity

To derive the marginal distribution of the instantaneous total intensity, convert to spherical coordinates using the Jacobian determinant,

$$\left| \frac{\partial (s_1, s_2, s_3)}{\partial (r, \theta, \phi)} \right| = r^2 \cos \phi \quad (\text{E14})$$

to arrive at the joint density,

$$f(r, \theta, \phi) = \frac{r \cos \phi}{\pi S^2} \exp \left[-2 (S_0 r - |\mathbf{S}| r \cos \phi \cos \theta) / S^2 \right]. \quad (\text{E15})$$

Note that $r = s_0$ and integrate over θ and ϕ (see [Equation19.nb](#)) to yield

$$f(s_0) = \frac{2}{|\mathbf{S}|} \exp \left(-2 \frac{S_0}{S^2} s_0 \right) \sinh \left(-2 \frac{|\mathbf{S}|}{S^2} s_0 \right). \quad (\text{E16})$$

In terms of the eigenvalues,

$$f(s_0) = (\lambda_0 - \lambda_1)^{-1} \left[\exp(-\lambda_0^{-1} s_0) - \exp(-\lambda_1^{-1} s_0) \right]. \quad (\text{E17})$$

This distribution has mean S_0 and variance $\|S\|^2/2$.

E.2. Equation (20): Instantaneous Major Polarization

To derive the marginal distribution of the major or natural polarization, convert to cylindrical coordinates using the Jacobian determinant,

$$\left| \frac{\partial (s_1, s_2, s_3)}{\partial (t, \theta, s_1)} \right| = t \quad (\text{E18})$$

to arrive at the joint density,

$$f(t, \theta, s_1) = \frac{t}{\pi S^2 s_0} \exp \left[-2 (S_0 s_0 - |\mathbf{S}| s_1) / S^2 \right]. \quad (\text{E19})$$

Note that $s_0^2 = t^2 + s_1^2$ and integrate over θ and t (see [Equation20.nb](#)) to yield

$$f(s_1) = \frac{1}{S_0} \exp \left(-2 \frac{S_0 |s_1| - |\mathbf{S}| s_1}{S^2} \right). \quad (\text{E20})$$

In terms of the eigenvalues,

$$f(s_1) = (\lambda_0 + \lambda_1)^{-1} \begin{cases} \exp(-\lambda_0^{-1} s_1) & s_1 > 0 \\ \exp(\lambda_1^{-1} s_1) & s_1 < 0 \end{cases} \quad (\text{E21})$$

This distribution has mean S_1 and variance $\|S\|^2/2$.

E.3. Equation (21): Instantaneous Minor Polarization

This equation is derived in Appendix A of the paper. The equations in Appendix A are derived in [AppendixA.nb](#).

Note that this distribution has mean 0 and variance $S^2/2$.

E.4. *Sample Means*

The distribution of the sample mean degree of polarization, p , as a function of the number of samples, n , and the populations mean degree of polarization, P , are derived in Appendix B of the paper. The equations in Appendix B are derived in `AppendixB.nb`.

F. EQUATION (28): STOKES COVARIANCE MATRIX

F.1. *The short way*

For the simplest derivation of the covariance matrix, note the following:

- A unitary transformation does not alter the degree of polarization; therefore, \mathbf{b} must be Hermitian and $\mathbf{b}^2 = 2\rho$.
- The Mueller matrix \mathbf{B} of the Jones matrix \mathbf{b} is a Lorentz transformation, which is symmetric; therefore $\mathbf{C} = \mathbf{B}^2$.
- The Mueller matrix \mathbf{B}^2 corresponds to the Jones matrix 2ρ , which is also Hermitian; therefore, \mathbf{C} is also a Lorentz transformation.

Refer to Equation (12) of Britton (2000) for the axis-angle parameterization of a Lorentz transformation, and substitute the Jones matrix

$$\mathbf{B}_{\hat{\mathbf{m}}}(\beta) = 2\rho = S_i \sigma_i.$$

Here, it is useful to note that

$$\begin{aligned} \cosh 2\beta &= 2 \cosh^2 \beta - 1 = 2S_0^2 - 1 \\ \sinh 2\beta m_k &= 2 \cosh \beta \sinh \beta m_k = 2S_0 S_k \end{aligned}$$

F.2. *The long way*

Alternatively, you can start with the definition of the covariance matrix, $\mathbf{C} = \mathbf{B} \mathbf{B}^T$, or

$$C_{ij} = B_i^k B_j^k = \frac{1}{4} \text{Tr}(\sigma_i \mathbf{b} \sigma_k \mathbf{b}^\dagger) \text{Tr}(\sigma_j \mathbf{b} \sigma_k \mathbf{b}^\dagger) \quad (\text{F22})$$

and note that the trace is

- a scalar: $a = \text{Tr}(\mathbf{A})$;
- linear: $a \text{Tr}(\mathbf{B}) = \text{Tr}(a\mathbf{B})$;
- commutative: $\text{Tr}(\mathbf{AB}) = \text{Tr}(\mathbf{BA})$; and
- a projection operator: $\mathbf{A} = \text{Tr}(\mathbf{A} \sigma_i) \sigma_i / 2$.

Therefore,

$$C_{ij} = \frac{1}{4} \text{Tr} [\text{Tr}(\mathbf{b}^\dagger \sigma_i \mathbf{b} \sigma_k) \sigma_k \mathbf{b}^\dagger \sigma_j \mathbf{b}] \quad (\text{F23})$$

$$= \frac{1}{2} \text{Tr}(\mathbf{b}^\dagger \sigma_i \mathbf{b} \mathbf{b}^\dagger \sigma_j \mathbf{b}) \quad (\text{F24})$$

$$= 2 \text{Tr}(\sigma_i \rho \sigma_j \rho), \quad (\text{F25})$$

which is the Mueller matrix of 2ρ . Again, it is possible to refer to Equation (12) of Britton (2000) or use the trace of the anticommutator,

$$\text{Tr}(\{\mathbf{A}, \mathbf{B}\}) = 2 \text{Tr}(\mathbf{AB}) \quad (\text{F26})$$

to show that

$$C_{ij} = 2 \text{Tr}(\{\sigma_i \rho, \sigma_j \rho\}) = \frac{1}{2} S_k S_l \text{Tr}(\{\sigma_i \sigma_k, \sigma_j \sigma_l\}). \quad (\text{F27})$$

The anticommutator of the Pauli matrices,

$$\{\sigma_i, \sigma_j\} = 2\delta_{ij} \sigma_0. \quad (\text{F28})$$

Therefore, only 4 of the 16 terms in the above double sum do not vanish. When $i = j$, the four $k = l$ terms remain. If $i = j = 0$, the result is simply twice the Frobenius norm,

$$C_{00} = 2\text{Tr}(\boldsymbol{\rho}^\dagger \boldsymbol{\rho}) = S_k S_k = 2S_0^2 - |S| \quad (\text{F29})$$

For $i = j > 0$, two terms are positive and two are negative:

1. $k = l = 0$: $\text{Tr}(\{\boldsymbol{\sigma}_i, \boldsymbol{\sigma}_i\}) = 4$;
2. $k = l = i = j$: $\text{Tr}(\{\boldsymbol{\sigma}_0, \boldsymbol{\sigma}_0\}) = 4$;
- 3–4. otherwise: $\text{Tr}(\{i\epsilon_{ik\alpha}\boldsymbol{\sigma}_\alpha, i\epsilon_{ik\alpha}\boldsymbol{\sigma}_\alpha\}) = 4i^2 = -4$.

Therefore,

$$C_{\alpha\alpha} = S_0^2 + S_\alpha^2 - S_\beta^2 - S_\gamma^2 = 2S_\alpha^2 + |S|, \quad (\text{F30})$$

where α, β , and γ are all greater than zero and unequal. Combining the two equations yields

$$C_{ii} = 2S_i^2 - \eta_{ii}|S| \quad (\text{F31})$$

(no summation is implied by repeated indices). When $i \neq j$, the four terms that remain are

1. $k = i$ and $l = j$: the arguments to the anticommutator are the identity matrix and the trace is 4;
2. $k = j$ and $l = i$: if either i or j is zero, then the arguments to the anticommutator are the other matrix and the trace is 4; otherwise, $\boldsymbol{\sigma}_i \boldsymbol{\sigma}_j = -\boldsymbol{\sigma}_j \boldsymbol{\sigma}_i = i\epsilon_{ijk}\boldsymbol{\sigma}_k$ and the trace is $-4i^2 = 4$.
3. $k = 0$ and $\epsilon_{jli} \neq 0$: $\text{Tr}(\{\boldsymbol{\sigma}_i, \pm i\boldsymbol{\sigma}_i\}) = \pm 4i$;
4. $l = 0$ and $\epsilon_{ikj} \neq 0$: $\text{Tr}(\{\mp i\boldsymbol{\sigma}_j, \boldsymbol{\sigma}_j\}) = \mp 4i$.

The last two terms cancel each other, and $C_{ij} = 2S_i S_j$.

F.3. In the Eigen Basis

In the eigen basis, the covariance matrix

$$\mathbf{C} = \begin{pmatrix} S_0^2 + |\mathbf{S}|^2 & 2S_0|\mathbf{S}| & 0 & 0 \\ 2S_0|\mathbf{S}| & S_0^2 + |\mathbf{S}|^2 & 0 & 0 \\ 0 & 0 & S^2 & 0 \\ 0 & 0 & 0 & S^2 \end{pmatrix} \quad (\text{F32})$$

from which it is trivial to derive the determinant by Laplacian expansion,

$$|\mathbf{C}| = (S_0^2 + |\mathbf{S}|^2)^2 S^4 - (2S_0|\mathbf{S}|)^2 S^4 = S^8 \quad (\text{F33})$$